ELSEVIER

Journal of Power Sources 112 (2002) 353–366

JOURNAL OF POWER SOURCES

www.elsevier.com/locate/jpowsour

Nickel–zinc accordion-fold batteries with microfibrous electrodes using a papermaking process

Wenhua H. Zhu*, Mark E. Flanzer, Bruce J. Tatarchuk

Department of Chemical Engineering, The Center for Microfibrous Materials Manufacturing, Auburn University, Auburn, AL 36849, USA

Received 1 July 2002; accepted 22 July 2002

Abstract

Thin microfibrous substrates were built using a low cost, high speed, wet lay papermaking process with nickel and copper microfibers. High quality microfiber sheets with designed thickness and void volumes were fabricated at the Center for Microfibrous Materials Manufacturing at Auburn University. Products include thin microfibrous nickel and copper substrates with or without suitable expanded metal meshes, either sandwiched inside or on the backside. An improved method for fabrication of zinc electrodes was accomplished by electro-depositing active zinc material on 6 and/or 9 μm diameter microfibrous copper substrates. These zinc electrodes with various additives were examined for shape change and tested for performance. A new structure of electrode design was employed using an accordion-fold cell. By using five individual segments sintered onto an expanded metal mesh, an accordion-fold cell (670 mAh rated capacity) was assembled and had 98.0% coulomb efficiency, 88.6% energy efficiency at 72% depth-of-discharge (DOD) and 73.2% state-of-recharge (SOR) in the 79th cycle. A Ni–Zn cell consisting of one thick nickel and one thick zinc electrode was tested for rate performance in comparison with the 670 mAh accordion-fold cell. The accordion-fold cell (1279 mAh rated capacity) was scaled-up and tested for 835 cycles at 38% DOD at a 0.3 C charge and discharge rates, and continuously operated at 38% DOD until the 1050th cycle was finished at 0.16 C charge/discharge rates. A 7115 mAh accordion-fold demonstration cell was tested at 0.28 C charge and discharge rates for 608 cycles and still had a 4.7 Ah capacity at a 0.08 C discharge rate.

Keywords: Microfibrous copper materials; Zinc electrodes; Thin nickel electrodes; Secondary nickel zinc batteries

1. Introduction

Microfibrous metal materials are a relatively new development in battery applications. Several metal fiber manufacturers exist, such as Memtec America Corporation, Ribbon Technology Corporation, National Standard, and Micro-Metal Fibers Inc. and produce a variety of different metal types. Auburn University has developed a wet lay papermaking process to combine micron diameter metal fibers and cellulose fibers into non-woven preforms resembling sheets of paper [1,2]. Paper preforms are formed easily via an automated high speed continuous papermaking machine at the Center for Microfibrous Materials Manufacturing (CM^3) at Auburn University. Subsequent sintering in hydrogen at elevated temperatures in an industrial size continuous belt furnace removes the cellulose binder and sinter-locks the metal fibers together. Using this process, the University has fabricated and evaluated sintered metal fiber–carbon fiber composite structures for supercapacitors and fuel cells as well as sintered nickel fiber electrodes for nickel-based batteries.

Various related electrode structures have been developed in the past ten years at Auburn University [3–7]. Kohler et al. developed an approach to fabrication of composite carbon electrodes [3,4]. Johnson et al. produced a novel structure of nickel electrodes by coating nickel hydroxide onto small diameter nickel fibrous network [5].[1] The electrodes have features of high surface area, low weight, and uniform coating layer. Adanuvor et al. fabricated 2 μm diameter fibrous nickel electrodes and tested in flooded half-cell for more than 2090 cycles [6]. Flanzer [7] made thin microfiber-based zinc electrodes by using copper fibrous substrates.

Battery requirements for a zinc electrode include a high energy yield at high current densities. During repeated charge and discharge cycles, zinc electrodes have to possess good physical strength and integrity in order to withstand severe environmental stresses and in order to adequately retain their active material [8]. Most of the zinc

* Corresponding author. Tel.: +1-334-844-2026; fax: +1-334-844-2085.
E-mail address: whzhu@eng.auburn.edu (W.H. Zhu).

[1] Computer program caused the utilization error. It was fixed by Adanuvor et al. [6].

0378-7753/02/$ – see front matter
PII: S0378-7753(02)00446-9

electrodes are prepared as a mixture of Zn and/or ZnO powders with suitable additives [9]. Finely divided spongy or mossy zinc deposits were formed at low current densities when zinc deposition was made from alkaline zincate electrolyte [10,11]. Also, the addition of $Ca(OH)_2$ was used to trap soluble zincate within its structure. This resulted in the reduced shape change and longer cycle life (400–550 cycles to 70% of the theoretical cell capacity [12]. Charkey [13] developed a new technology of long cycle life sealed nickel–zinc batteries. The zinc active element was formed from ZnO, $Ca(OH)_2$, PbO, and PTFE. A gas recombination element comprised a sheet of plastic-bonded CdO. The zinc electrodes were fabricated by a plastic roll-bonding process, which consisted of two of the above elements attached to both sides of a silver-plated perforated copper foil. Cao et al. improved nickel–zinc deep-cycle-life performance through the development of a reduced solubility plastic bonded zinc electrode. Individual cells and battery modules achieved 600 cycles at 100% depth-of-discharge (DOD) while maintaining a high specific energy up to 60 Wh/kg [14]. Normally, metal grids are used as the support structure for zinc electrodes, serving also as current collectors. A new three-dimensional copper foam matrix was applied for retaining Zn/ZnO materials in order to improve the conductivity of the zinc electrode [15]. By using technology based on Auburn University's previous work involving fibrous nickel electrodes [5,6], a method of making zinc electrodes is presented by using microfibrous copper support materials through an electrochemical impregnation (ECI) process. The related results on testing zinc electrodes and scale-up of microfibrous electrode structure for Ni–Zn accordion-fold cells are described in this paper.

2. Experimental

2.1. Microfibrous support materials by paper-making process

Paper preforms were made on a lab scale with a circular preform having a diameter of 16 cm (201 cm^2 area). Fiber sheets were also made with square preforms of 1 ft^2 with an automated sheet mold machine. The porous substrate was formed using Auburn University patented technologies [1,2]. Well-blended small copper fibers along with cellulose fibers were collected on a sheet mold to form a wet paper composite preform. The pressed and dried preform was then sintered in a hydrogen-reducing atmosphere. Paper preforms were successfully sintered to give a three-dimensional fibrous structure of high surface area. The pilot scale furnace has a typical belt speed of 4.4 in./min, resulting in a sintering time of 45 min. Electrodes were sintered onto expanded metal foils, such as a 1.5 mil thick Delker screen, for mechanical strength and better current distribution.

2.2. Thin nickel electrodes

Nickel electrode substrates consisted of one layer of preform sintered together with an expanded nickel foil on one side. Larger 4 μm (50 wt.%) diameter nickel fibers were added to 2 μm nickel fibrous structure because larger diameter fibers increased the substrate strength and reduced electrode corrosion with minimum impact on performance. The cellulose fibers were employed as a binder to form the paper preform in the manufacturing process. The microfibrous sheets were scaled to 1 ft^2 with a sheet forming paper machine. The whole process was automated via the Center for Microfibrous Materials Manufacturing Facility at Auburn University.

The nickel/cellulose preforms were sintered in an industrial-sized furnace at temperatures from 925 to 1125 °C. After sintering, the microfibrous substrates were pretreated in an ultrasonic deionized water bath (FS-14 Ultrasonic Cleaner, Fisher Scientific) in order to eliminate surface contaminants. Wet oxidation [16] was used for cleaning the substrate surface and reducing surface corrosion during the electrochemical impregnation process. The pretreated substrates were weighed, measured, and forwarded to the ECI process. Nickel hydroxide electrodes were prepared in a bath consisting of 2 M $Ni(NO_3)_2$, 0.23 M $Co(NO_3)_2$ and 0.10 M $NaNO_2$. The electrode impregnation was conducted in a water-jacketed beaker (700 ml solution) at 90 ± 1 °C. The pH of the solution was initially adjusted to the desired value of 4.0 by adding ammonium hydroxide. A nickel wire was spot-welded to the fibrous substrate for connection to the power supply. Substrates were impregnated using multiple current steps until the targeted loading level between 1.1 and 1.9 g/cm^3 void was obtained. After impregnation, each electrode was rinsed in deionized water and then dried at 60 °C for at least 4 h.

Nickel electrodes after drying were then soaked in 26% KOH for at least 4 h. Next, the electrodes were formed using eight cycles of 20 min charge and 20 min discharge at a 70 mA/cm^2 current density in 26% KOH solution [17,18]. After the formation process, the electrodes were completely rinsed with deionized water until the pH value of the washing solution was neutral. Formed electrodes were dried at 60 °C for at least 4 h and weighed to determine the theoretical capacity using the electrochemical equivalent of 289 mAh/g of the nickel hydroxide based on one electron transfer involved in the cell reaction.

2.3. Thin zinc electrodes

Copper was determined to be one of the best metals for use as a zinc electrode substrate by a corrosion study [7]. Copper fibers have diameters of 2, 6, and/or 9 μm and a length of 2 mm, obtained from Micro-Metal Fibers. The estimated fiber cost on a weight basis was approximately the same for copper and nickel fibers, but copper fibers had superior qualities. Microfibrous substrates consisted of 6 and

9 μm diameter copper fibers with loadings of approximately 50% each, sintered together onto an expanded copper foil on one side. The larger diameter fibers were less expensive, but the 6 μm smaller copper fibers were added for increasing electrode surface area.

Paper preforms were successfully sintered to form microfibrous network structures. Copper fiber substrates were obtained after the preforms were sintered in either a lab scale furnace or a pilot scale belt furnace at typical temperatures ranging from 800 to 1000 °C in a hydrogen environment. The methods for depositing active zinc (zinc/zinc hydroxide) onto microfibrous copper substrates included direct electroplating, physical pasting and electro-precipitation. Electroplating was conducted using alkaline zincate electrolytes whereas the ECI process was performed using a zinc nitrate (1.6 M $Zn(NO_3)_2$ and 0.1 M $NaNO_2$) solution in a water-jacketed beaker (700 ml solution) at 90 ± 1 °C. Direct electroplating produced mossy zinc depositions that usually clogged the void spaces of microfibrous substrates, which consisted of sintered copper fibers with 6 μm diameter. In comparison, electro-precipitation of $Zn(OH)_2$ resulted in more conformal coatings, maintaining the structural integrity of the electrodes. Furthermore, additives, such as calcium, cadmium and/or lead in the form of their metal salts were incorporated into the electro-precipitation baths in order to increase the cell rate and cycle performance. The theoretical capacity of the zinc electrode was evaluated using the electrochemical equivalent of 539.4 mAh/g of the zinc hydroxide based on two-electron transfer involved in the cell reaction.

2.4. Ni–Zn accordion-fold cells

A new electrode design, using segmented sections sintered onto an expanded metal mesh, was used in the substrate making for setting up accordion-fold cells. This improved design allowed for easy folding of the electro-precipitated materials and prevented shorting between the electrodes that occurred at the folds with the non-segmented microfibrous structures. Two and 4 μm microfibrous nickel substrates with 20 mm × 60 mm segmented sections were electrochemically impregnated with a targeted amount of nickel hydroxide active material, normally at a loading level of 1.6–1.8 g/cm^3 void. Small amounts of cobalt were simultaneously deposited by incorporating 10% (B.M.) cobalt nitrate in the impregnation bath.

After microfibrous substrates were loaded with the active materials, the electrodes were usually activated through an eight-cycle formation. These segmented nickel electrodes were washed completely and then dried at 60 °C for a minimum of 4 h. Resulting advantages of these electrodes were higher rates and longer cycle life performance with lower loss of active material during the cycling test. A zinc electrode with five segments was made by a similar method to the above nickel electrode.

The accordion-fold cells of initial work shorted due to contact of the positive and negative electrodes at the folding edges, leads or tabs, which produced extremely low discharge energy after the cell charge. Later, five individual nickel fiber preforms (20 mm × 60 mm) were sintered onto an expanded nickel mesh (65.0 mm × 107.5 mm, 1.5 mil thick). After sintering, the fiber substrate thickness was 17 mil. The copper substrate was made from 6 μm copper fiber and had a thickness of 8 mil. After zinc coating and electro-deposition, the thickness of zinc electrode increased to 11.8 mil. The zinc capacity was calculated by assuming that all deposition on the fiber network was zinc hydroxide.

Both nickel and zinc electrodes made by electro-deposition were very brittle after the precipitation process. It became a problem during assembling and testing of the accordion-fold cell. The electrode formation process before cell assembly softened the long strip of nickel material, and this allowed successful multiple folding. For the formation process, the zinc electrodes were tested in 5% KOH, 26% KOH, and the NCP solutions. Different weight loss of zinc active material existed because of dissolution in the alkaline electrolyte. Limited charge to the zinc electrode in the half-cell for a short 30 min made the zinc electrode soft for folding.

For a nickel–zinc cell in the cycle test, the rated capacity was obtained by using the maximum cell capacity measured at a specified lower discharge rate at room temperature. It was applied to calculate the depth-of-discharge and the cycle current at various charge and discharge rates.

2.5. Cell construction

Test cells were constructed of polymethylmethacrylate (PMMA), a material resistant to KOH. Cut outs were made to dimensions slightly larger than the electrodes used for testing, typically 20 mm × 60 mm or 40 mm × 60 mm. By obtaining the thickness of the individual components and the total cell thickness, the 'pocket' depths were determined. A variety of EPDM gaskets with different thickness were employed to give flexibility to the cell design with respect to changing electrode thickness. The gasket also provided a suitable seal when the cell was clamped together. Plate or U-type clamps were used to ensure an even pressure along the entire length of the cell, and these clamps also allowed easy assembly and disassembly. The cell utilized a pressure gauge (0 to 15, −30 to 150, or −30 to 300 psi) to monitor accumulating gas pressure. Fig. 1 illustrates how the cell was assembled including the order of each component. Much care was needed during assembly to ensure proper alignment of electrodes, wicking material, and separator. A small thread hole was drilled into the PMMA wall for feeding electrolyte and removing gas during cell formation. The cells were then sealed with a screw wrapped with a Teflon tape.

Separators were used in nickel–zinc cells to retard zinc dendrite penetration and also to prevent the electrodes from

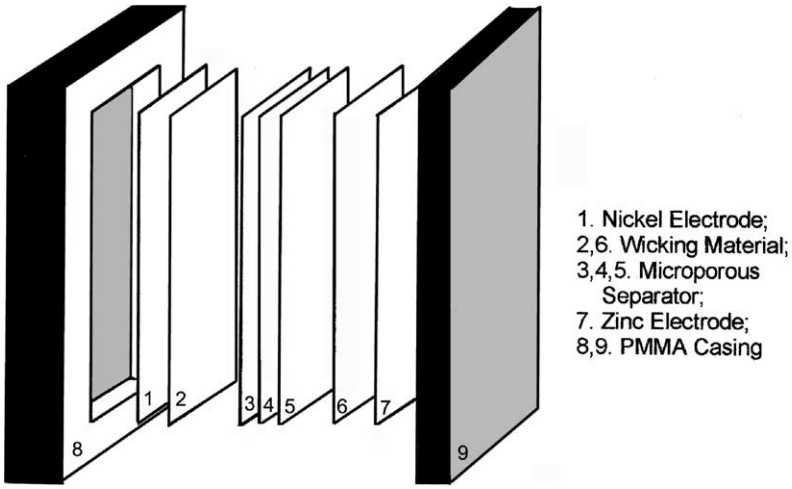

Fig. 1. Schematic view of the Ni–Zn test cell including casing, electrodes, wicking material, and separator.

shorting. Celgard 3401 (Hoechst Celanese Corp.) microporous membranes were chosen for the purpose of providing physical separation of electrodes while keeping ionic conductivity intact. The membrane is an opaque microporous film made from polypropylene and polyethylene resins. They have excellent resistance to acids, bases, and most chemicals, and hence provide long-term stability in batteries. Hydrophilic in nature, Celgard 3401 membranes are manufactured from a base membrane (Celgard 2400) having hydrophobic properties. Electrode wetting was improved by placing one layer of a non-woven fibrous material next to each electrode. The wicking material was Pellon 2517 (Freudenberg Nonwovens, Chelmsford, MA), a non-woven polyamide.

For single cell tests, all electrodes and peripheral materials were fully wetted in the NCP electrolyte. All weights of dry and wet materials were recorded. Excess electrolyte was allowed to drip off and then the cell was assembled. Electrolyte was added and then the cell placed in a dessicator under vacuum to get rid of air pockets inside. A nickel electrode and a zinc electrode with segmented sections, separated by a separator group, were folded to form an accordion-fold cell as shown in Fig. 2. As a cell separator, there were three layers of Celgard 3401 between two layers of Pellon 2517 wicking materials. The 7115 mAh accordion-fold cell is shown in Fig. 3. The electrolyte saturation level (ESL)[2] used in the sealed cell was 70–100%. Assembled cells were tested by a battery test system (Arbin Instruments).

2.6. Gas recombination design

Cadmium promotes the catalytic and chemical recombination of oxygen during charge and discharge of the cell [13]. For a sealed cell to function properly, gases generated during the end-of-charge and overdischarge must be recombined within the cell. Unlike with nickel–cadmium batteries, the use of membrane separators (two layers of Pellon and three layers of Celgard) in nickel–zinc cells limited the transport and access of oxygen to the zinc electrode for

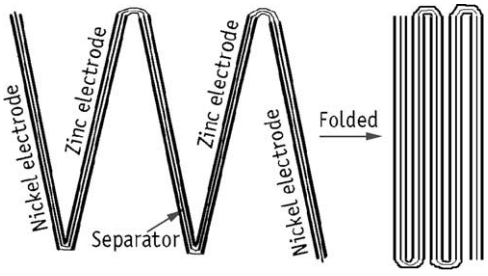

Fig. 2. Schematic drawing of the accordion-fold Ni–Zn cell.

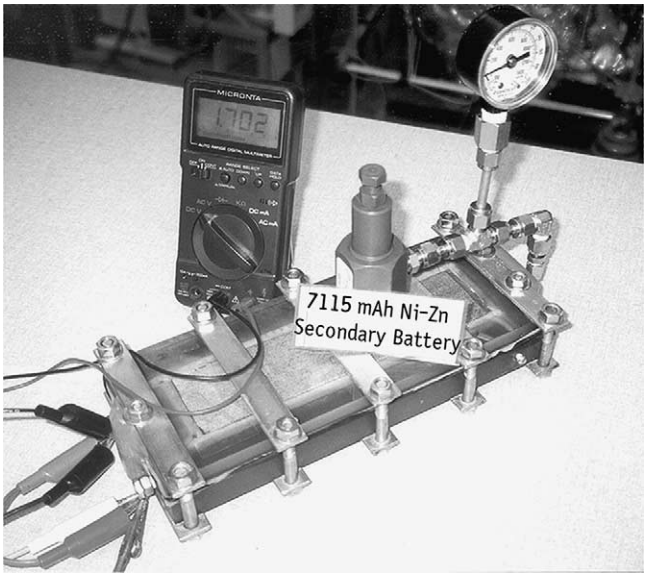

Fig. 3. Photograph of sealed accordion-fold Ni–Zn cell during discharge. Sample NiZn-20, six accordion folds, and 7115 mAh rated capacity.

[2] Each component including electrodes and separators has its own void volume. The definition of 100% electrolyte saturation level is that the whole void volume of all components is fully filled with electrolyte.

direct recombination. Therefore, the recombination rate in the nickel–zinc cell was much lower than that in the sealed nickel–cadmium cell. The original accordion-fold design for sealed cells improved oxygen management because of its wound structure, and solved the problem of oxygen permeation in several layers of microporous membranes in sealed nickel–zinc cell. Lower oxygen evolution from the positive electrode during the end-of-charge was recommended for the nickel–zinc cell. Oxygen evolution especially during overdischarge was related to the cycle life of the nickel electrode and acceleration of the passivation of zinc electrode. Cadmium was a good additive for increasing hydrogen overpotential, improving oxygen management, reducing zinc shape change and prolonging the cycle life although it reduced coulomb efficiency and energy efficiency of the nickel–zinc cell.

Small amounts of hydrogen created by the zinc electrode corrosion and evolved from the cell charge are necessary to recombine in the sealed nickel–zinc cell. The principle of the nickel–hydrogen cell is used here for hydrogen management, i.e. one gas diffusion electrode connected to the working nickel electrode consists of a small gas-recombination Ni–H_2 cell and avoids hydrogen pressure build-up.

2.7. Cycle test and cell reconditioning

For the simple nickel–zinc cell, a test procedure was developed for cycle testing of nickel–zinc cells. First, current values were determined based on rates and the cell rated capacity. The cell was assembled in its fully discharged state by using the $Zn(OH)_2$ electro-precipitated electrode and the nickel electrode. The first step charged the cell to 66% of the available zinc capacity at a low current. To achieve this, a constant current was applied until a cell voltage of 1.93–1.95 V was reached. The step was then switched to constant voltage mode until the cell received the designed charge acceptance. The cell then began its cycle test by discharge/charge. The cell was discharged to a specified capacity or cut-off voltage, and then charged to a level of SOR for the cell able to cycle at a specified depth-of-discharge. If the voltage became greater than the specified maximum voltage during the constant current charge, the charging mode was switched to a constant voltage until the complete charging capacity was obtained. This was done to prevent a voltage excursion and dendrite formation. The charging and discharging procedures were repeated until the cell degraded to the end-of-life (EOL) definition for the cycle test.

A test protocol was improved for cycle test in the accordion-fold cell. Before cell cycling, the zinc electrode needed to be charged with a lower current (0.1 C rate) to one-third of the available zinc capacity. Cell formation was then performed three times with gradually increased capacity each time. After the formation process, the cell started a normal cycle of charge and discharge. The state-of-recharge (SOR, i.e. recharge factor) based on the cell rated capacity was chosen from 74.6 to 78.4% for the NiZn-05 cell as shown in Table 1. This was done to decrease the rate of oxygen evolving from nickel electrode at 72% DOD.

Table 1
Cycle regime of 670 mAh five-accordion-fold nickel zinc cell (sample NiZn-05)

Cycle description	Parameters
Charge at 0.3 C from 74.6 to 78.4% state-of-recharge (SOR)	200 mA charge input from 500 to 525 mAh
Discharge at 0.3 C to 72% depth-of-discharge (DOD)	200 mA discharge output to 480 mAh
End-of-life test definition (cell capacity is unrecoverable)	Cycle failed if the cell discharged to 1.45 V cut-off voltage and the cell capacity less than 480 mAh

For electro-deposited nickel and zinc electrodes in the accordion-fold cell, the accumulating coulomb efficiency of nickel electrode was higher than the zinc electrode especially in the initial stage, because the nickel electrode was well formed outside the cell. Furthermore, a small amount of hydrogen evolution, zinc electrode passivation and shape change reduced the efficiency of the zinc electrode. This resulted in an increase of oxygen evolution from nickel electrode. Once some oxygen evolved in the sealed cell, the cell capacity reduced gradually due to zinc oxidation. As a whole, there was a significant disparity between the charging efficiencies of the nickel and zinc electrodes.

The cell reconditioning was important to keep the accordion-fold cell working. There were several ways to recover or maintain a charge balance between the electrodes in the nickel–zinc cells. The first one was to charge the cell to approximately 90% SOR at a 0.2–0.4 C rate and then discharge the cell at 0.1 C rate to the 1.2 V cut-off voltage. This dropped the state-of-charge (SOC) level of the nickel electrode. Secondly, an additional thin nickel electrode was used as a counter-electrode for discharging the working nickel electrode to obtain a charge balance. Thirdly, an additional hydrogen electrode consumed some nickel electrode capacity when it performed gas management. This method prolonged the time requiring for balancing the two electrodes and reconditioning the cell.

3. Results and discussion

3.1. Microstructure of preforms, fibrous substrates and electrodes

The larger cellulose fibers were employed as a binder to form the paper preform in the manufacturing process [1,2]. The sintered three-dimensional structure with characteristics of high surface area, low weight, and favorable electrical conductivity can be used for improving the specific capacity of the nickel and zinc electrodes. The SEM micrograph of a

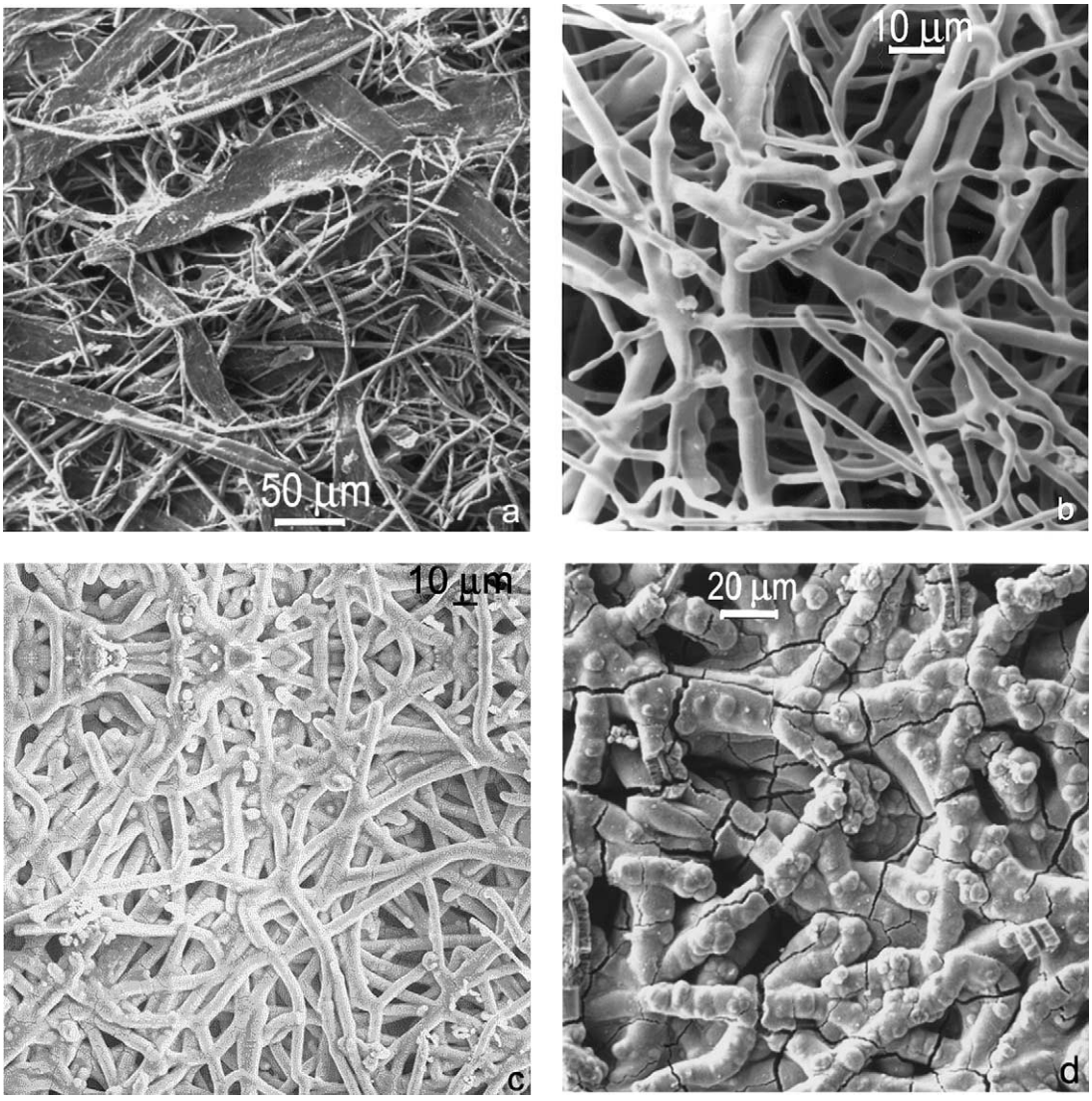

Fig. 4. Scanning electron micrographs of Auburn preform, substrate and microfibrous nickel electrode. (a) Preform made from 2 and 4 μm nickel fiber and cellulose fiber; (b) sintered substrate images of 2 and 4 μm mixed diameter nickel fiber; (c) Auburn microfibrous nickel electrode; (d) tested nickel electrode made from 2 and 4 μm mixed diameter fibers.

composite sheet, Fig. 4a, shows a preform microstructure containing 2 and 4 μm nickel and cellulose fibers with a loading of 50% metal and 50% cellulose. The cellulose was gasified during the sintering process to create a high void volume structure. SEM micrographs of sintered fiber substrates are shown in Fig. 4b. The small diameter-mixed nickel fibers shown in the Fig. 4b are well sintered at their contact points to form an interlocking metal network. The SEM images of impregnated nickel electrodes are shown in Fig. 4c. Fig. 4d shows one of the electrode structures after test. The thickness of the coating layer was between 4.7 and 5.9 μm on 2 μm nickel fibers. The small three-dimensional network structure improved electrolyte management and increased the rate capability of the electrode.

Copper fiber substrates consist of 6 and 9 μm copper fibers sintered together with an expanded copper foil on one side as shown in Fig. 5a. For reducing the electrode cost, 9 μm copper fibers are added to fiber mixtures for making zinc electrodes. Small diameter copper fibers are used for increasing electrode surface area. Two types of preform composition and copper substrate parameters are given in Table 2. Small fibers with proper protection of coating/plating layer increase the contact surface area of active material to the current collector. Fig. 5b–d shows the structure of zinc electrodes with calcium additive. The zinc electrode was made with 30 μm coating layer of zinc materials at 20 mA/cm^2 in 30 min (Fig. 5b and c). The SEM pictures show that the electrochemical impregnation provides a possibility for making a composite structure of zinc electrode. The zinc electrode with calcium additive can be operated at a low-lever solubility or a relative insoluble state.

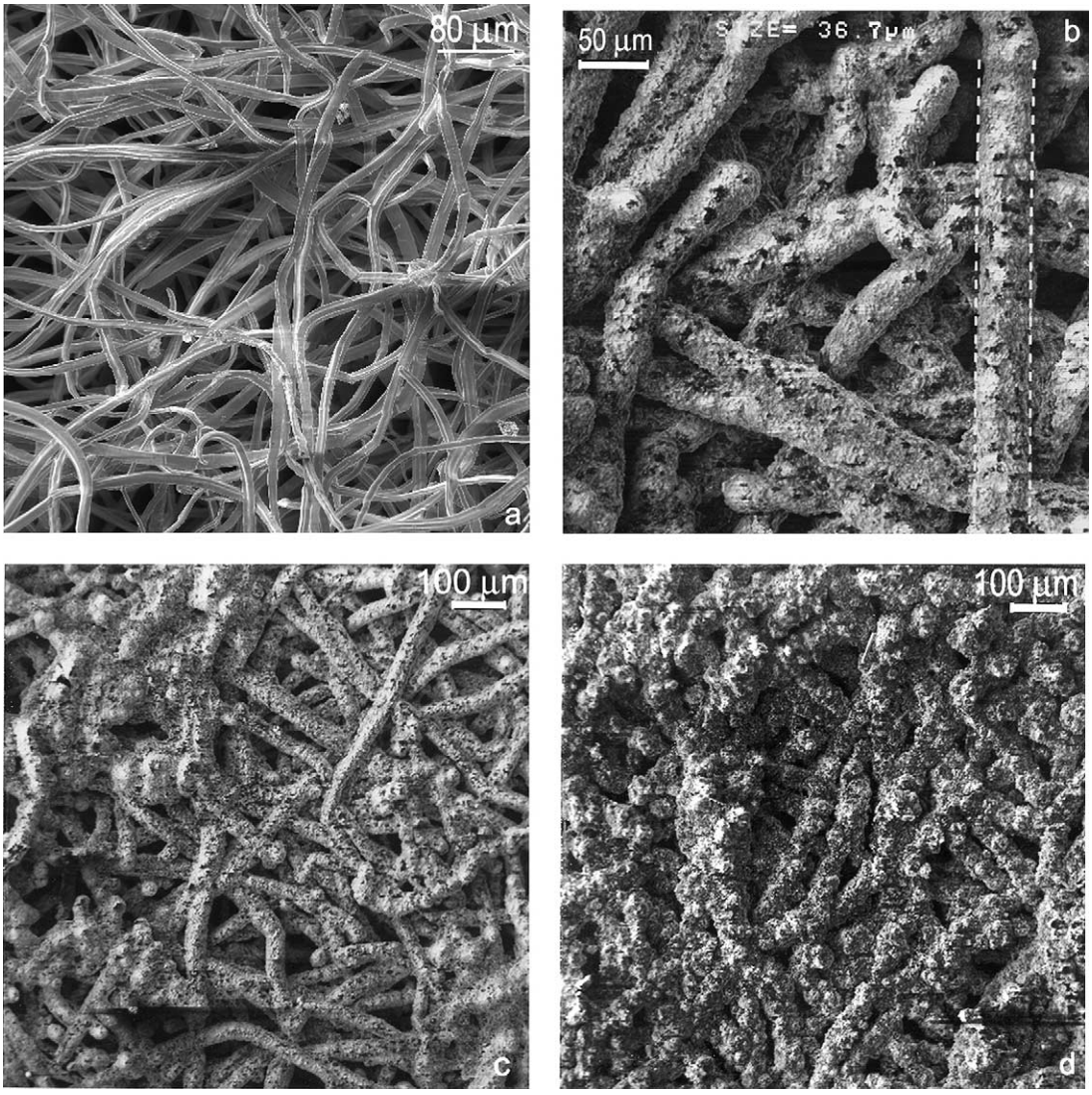

Fig. 5. SEM images of Auburn copper substrates and novel zinc electrodes with zinc hydroxide and additive. (a) Six and 9 µm mixed diameter copper fiber substrate; (b and c) zinc electrode deposited with Zn 1.6 M and Ca 0.788 M nitrate solution at 20 mA/cm^2 for 30 min, substrate plated; (d) zinc electrode deposited with Zn 1.6 M and Ca 0.788 M nitrate solution at 10 mA/cm^2 for 100 min, substrate plated.

3.2. Effect of additives on zinc electrodes

Physical mixing of zinc active materials and additive is a popular way for addition of additive to the zinc electrode. The electrochemical impregnation method is one of the methods for making nickel electrode. This impregnation technique was extended here for development of microfibrous zinc electrodes. Two steps of the following electrochemical and chemical reactions occur during the process,

$$NO_3^- + 7H_2O + 8e^- \rightarrow NH_4OH + 9OH^-, \quad E^\circ = -0.875\,V \tag{1}$$

$$Zn^{2+} + 2OH^- \rightarrow Zn(OH)_2\downarrow, \quad K_{sp} = 1.2 \times 10^{-17} \tag{2}$$

Table 2
Copper substrate compositions and parameters before and after sintering

Substrate	Fiber diameter (µm) and compositions	Preform compositions before sintering [Cu (%)/cellulose (%)] (mg/cm^2)	Substrate porosity (%)	Electrode thickness (mm)
SCU1	2, 6, and 9 (one-third for each)	[67.2/32.8] (0.0145/0.0071)	91.6	0.34
SCU2	6 and 9 (one-half for each)	[74.8%/25.2%] (0.0149/0.0050)	86.7	0.30

Zinc hydroxide precipitates when the ion solubility product exceeds its K_{sp} constant [19]. At meantime, zinc ion is also possibly reduced as follows:

$$Zn^{2+} + 2e^- \rightarrow Zn, \quad E^\circ = -0.763\,V \tag{3}$$

There is a 112 mV potential difference between reactions (1) and (3). Theoretically, the reduction reaction (3) of zinc ion is easier than the nitrate ion reduction (1). If the acidity of the impregnation solution is rather low, zinc particles deposit on the electrode surface. Formation of either Zn or $Zn(OH)_2$ on the microfibrous surface is decided by whether Zn^{2+} diffuses to the cathode surface or precipitate when it meets hydroxyl ions. Due to oxidation of the porous wet zinc in air, the surface color of zinc electrode pictures (Fig. 5b–d) turns white. Small dark particles on the surface are possibly the lead deposits. When zinc hydroxide is saturated in the impregnation nitrate solution, the surface color also turns white due to the precipitation of zinc hydroxide according to the reactions (1) and (2). The ratio of the chemical $Zn(OH)_2$ precipitation to the electrochemical zinc particle deposition needs further extensive work. The reduction potentials of Cd^{2+} and Pb^{2+} ions are rather positive to Zn^{2+}, So most of them will deposit to form a metal film first. The additives greatly prevent copper microfibrous substrate from corrosion during the cell cycle test.

$$Cd^{2+} + 2e^- \rightarrow Cd, \quad E^\circ = -0.403\,V \tag{4}$$

$$Pb^{2+} + 2e^- \rightarrow Pb, \quad E^\circ = -0.126\,V \tag{5}$$

During the ECI process, calcium hydroxide can co-precipitate with zinc hydroxide.

$$Ca^{2+} + 2OH^- \rightarrow Ca(OH)_2\downarrow, \quad K_{sp} = 5.5 \times 10^{-6} \tag{6}$$

Calcium hydroxide is added to zinc electrodes for improvement of shape change and dendrite growth [12]. This results in formation of insoluble calcium zincate $CaZn_2(OH)_6{\cdot}2H_2O$ [20]. If calcium zincate is assumed to be an active material, one may conclude that the zinc electrode discharge reaction is

$$2Zn(s) + Ca(OH)_2(s) + 4OH^- + 2H_2O \rightarrow CaZn_2(OH)_6 \cdot 2H_2O(s) + 4e^- \tag{7}$$

Here 's' represents solid. The electroprecipitation process was tried to form a proper coating film and produce a co-precipitated calcium zincate structure. When the ECI process was conducted in Zn 68%, Ca 29% and Cd 3% (B.M.) nitrate solution, the zinc electrode with conformal structure did not work in the NCP electrolyte cell (a patented electrolyte formulation, US Patent 5,215,836, NCP Inc.). When made in Zn 90%, and Cd 10% (B.M.) nitrate solution, the zinc electrode with high void structure also failed due to the lower zinc capacity. In fact, the cadmium ion is easier to reduce than the zinc ion (reactions (3) and (4)). Hence, the composition of the electro-precipitation solution was adjusted. When the zinc electrode was made in a Zn 98.35%, Cd 1.28% and Pb 0.37% (B.M.) nitrate solution, the zinc electrode formed with mossy structure was unsuccessful in the test nickel–zinc cell. When it was made in Zn 99.88%, and Cd 0.12% (B.M.) nitrate solution, the zinc electrode with a denser structure was successfully tested in the nickel–zinc cell. Another similar zinc electrode was finished by post-electrodeposition in 1.8 M cadmium nitrate for 15 min. The above two zinc electrodes were tested in the 1200 mAh cells. Both the cells were cycled more than one hundred times. The cadmium surface coating was designed to improve the zinc shape change and promoted oxygen recombination. As demonstrated by the tested open cell, small amounts of cadmium additive greatly protected the copper substrate from corroding, although it also reduced the cell energy efficiency. The test cells with the calcium/cadmium and calcium/lead additive failed to perform the cell cycle test in the NCP electrolyte. For the zinc electrode with calcium additive, 20% KOH was chosen to replace the NCP electrolyte in the nickel–zinc cell.

Scanning images of tested and untested zinc electrodes (nos. 1–13, images were scanned after nine cycles; nos. 14 and 15, original electrodes) are shown in Fig. 6 (HP 6270A scanner). Tested zinc electrodes (nos. 1–7) were physically made by paste-pressing technique. Other zinc electrodes were impregnated with zinc hydroxide and additive by electrochemical precipitation. The compositions of original electrodes are listed in Table 3. Sample ZN9014 was an untested electrode without any additive. Sample ZN9015 was an untested zinc electrode with calcium additive and had a uniform structure. Illustrations as shown in Fig. 6 (nos. 3–7, 10, 12, 13 and 15) demonstrated that calcium is an effective additive for improvement of zinc electrode shape change. The electrode capacity and rate performance are listed in Table 4. The addition of calcium and graphite reduced the electrode capacity (samples ZN9003, ZN9006, ZN9007, and ZN9013). Lead plating, lead and graphite addition were beneficial for higher rate performance. Single calcium additive decreased zinc utilization, but also reduced the shape change of zinc electrode.

3.3. Thin electrode accordion-fold cell and thick electrode single cell

Nickel and zinc electrodes in the NiZn-05 five-accordion-fold cell (Table 5) had total electrode thickness of 2.16 and 1.5 mm, respectively. After zinc metal plating, the electrodeposition was difficult because of the clogs of the micropores. Hence, deposition was conducted without zinc plating on 1.5–2.0 mm thick copper substrates. In comparison with testing of accordion-fold Ni–Zn cell with thin electrodes, the NiZn-07 cell consisted of one 2.10 mm thick nickel electrode (728 mAh) and one 1.98 mm zinc electrode (2143 mAh). The zinc electrode was so thick that the maximum capacity obtained at 200 mA charge/discharge current was 182.2 mAh. Furthermore, measures to activate this kind of cell in 20% KOH solution failed. This was related to most of the zinc hydroxide deposited inside the micropores of the

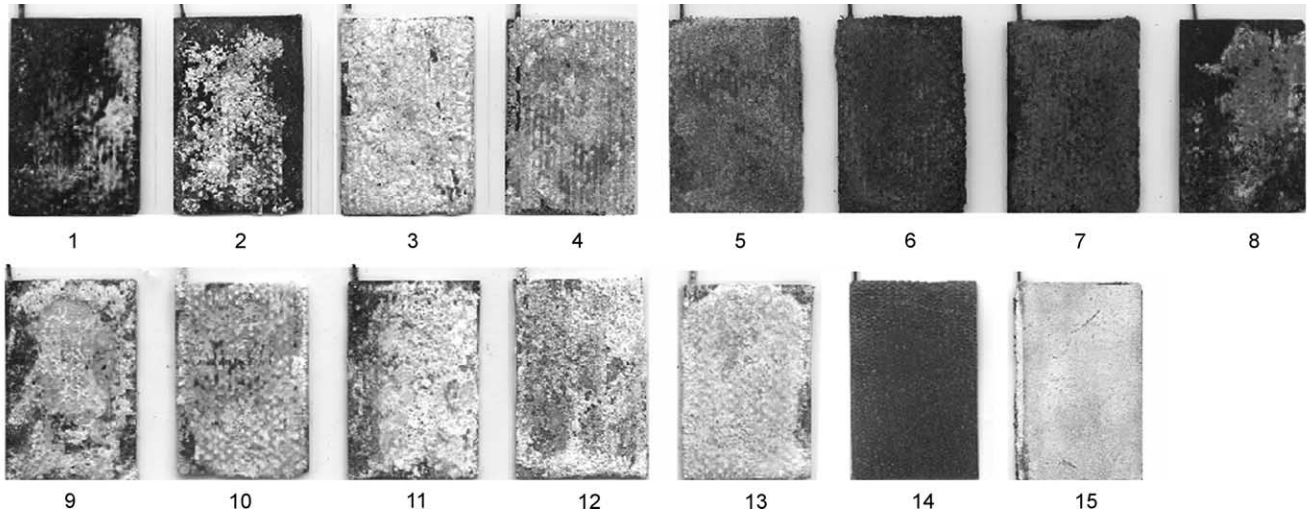

Fig. 6. Scanning photograph of various zinc electrodes made from paste technology (1–7) and electrochemical deposition (8–15). Electrodes nos. 1–13 were tested for formation and rate capability; electrodes nos. 14 and 15 are original samples made from different electrodeposition solutions and electrode no. 15 is a relatively insoluble zinc electrode with calcium additive.

copper substrate. The conformal dense structure of the zinc electrode made it difficult to wet zinc hydroxide inside the pores. Since the thick zinc electrode was not activated, a continuous strip (100 mm × 60 mm) of 6 μm copper substrate was electro-deposited to form a five-fold-thick zinc electrode (1.98 mm, 1675 mAh). This zinc electrode was similar to use in the NiZn-05 accordion-fold cell. The folded "thick" zinc electrode took the place of the above zinc electrode (2143 mAh) applied to make up a sample NiZn-07a cell.

The capacity reached a maximum value of 482.9 mAh when the charge input was 550 mAh at 120 mA charge/discharge current. The charge acceptance of the cell decreased with an increase of the charge rate at a fixed 200 mA discharge current. Furthermore, the discharge capacity was reduced with an increase of discharge rate at a 200 mA charge current. Therefore, the thick electrode cell with similar design capacity was more difficult to charge and discharge than the thin electrode accordion-fold cell. This means the thick electrode cell had a poorer rate capability. The performance comparison is listed in Table 6. The results demonstrate that the accordion-fold cell has better rate capability and a longer cycle life. From observation of the tested cell, the shape change (i.e. redistribution) of the zinc electrode reduced its rate capability and accelerated zinc electrode passivation. Furthermore, the loss of zinc electrode capacity accelerated the capacity build-up of nickel electrode and eventually caused the nickel–zinc cell to fail. Therefore, cell reconditioning for capacity balance was determined to be important for cell maintenance.

Table 3
Compositions of zinc electrodes made from 6 μm diameter copper fibrous substrates

Electrode no.	Compositions
(A) Paste zinc electrodes by slurry coating on copper fibrous substrate	
ZN9001	ZnO (0.2278 g) 98%, PTFE 2%; substrate without plating
ZN9002	ZnO (0.2278 g) 98%, PTFE 2%; substrate with lead plating at 2 mA/cm^2 for 12 min first
ZN9003	ZnO (0.2278 g) 73.5%, CaO 24.5 %, PTFE 2%; substrate without plating
ZN9004	ZnO (0.2278 g) 52.4%, CaO 17.9%, Cu 27.7%, PTFE 2%; substrate without plating
ZN9005	ZnO (0.2278 g) 65.9%, CaO 22.0%, PbO 10.1%, PTFE 2%; substrate without plating
ZN9006	ZnO (0.2278 g) 49.0%, CaO 16.4%, Graphite 32.6%, PTFE 2%; substrate without plating
ZN9007	ZnO (0.2278 g) 50.7%, CaO 16.9%, Graphite 17.0%, Cu 13.5%, PTFE 2%; substrate without plating
(B) Zinc electrodes by electrochemical impregnation	
ZN9008	1.6 M $Zn(NO_3)_2$, 0.10 M $NaNO_2$, 10 mA/cm^2 for 90 min; substrate with lead plating at 2 mA/cm^2 for 12 min first
ZN9009	1.6 M $Zn(NO_3)_2$, 0.10 M $NaNO_2$, 10 mA/cm^2 for 180 min; substrate with lead plating same as above
ZN9010	1.6 M $Zn(NO_3)_2$, 0.394 M $Ca(NO_3)_2$, 0.10 M $NaNO_2$, 20 mA/cm^2 for 100 min; substrate with lead plating at 2 mA/cm^2 for 20 min first
ZN9011	1.6 M $Zn(NO_3)_2$, 0.10 M $NaNO_2$, 20 mA/cm^2 for 100 min; substrate without plating
ZN9012	1.6 M $Zn(NO_3)_2$, 0.394 M $Ca(NO_3)_2$, 0.10 M $NaNO_2$, 20 mA/cm^2 for 100 min; substrate without plating
ZN9013	1.6 M $Zn(NO_3)_2$, 0.788 M $Ca(NO_3)_2$, 0.10 M $NaNO_2$, 20 mA/cm^2 for 100 min; substrate with lead plating at 2 mA/cm^2 for 20 min first
ZN9014	1.6 M $Zn(NO_3)_2$, 0.10 M $NaNO_2$, 10 mA/cm^2 for 100 min; substrate without plating
ZN9015	1.6 M $Zn(NO_3)_2$, 0.788 M $Ca(NO_3)_2$, 0.10 M $NaNO_2$, 10 mA/cm^2 for 100 min; substrate without plating

Table 4
Zinc electrodes and rate performance made from 6 μm diameter copper fibrous substrates

Electrode no.	Capacity[a] (mAh)	Discharge rate					Charge input at a C/3 rate (mAh)
		0.3 C	0.69 C	1.0 C	1.5 C	2.0 C	
(A) Paste zinc electrodes by slurry coating on copper fibrous substrate							
ZN9001	106.3	88.3	71.7	48.7	50.9	49.0	100
ZN9002	125.8	97.1	96.7	87.3	80.5	80.4	100
ZN9003	88.5	83.7	73.7	76.7	82.5	90.0	100
ZN9004	127.6	88.8	74.4	78.2	72.3	70.9	100
ZN9005	114.8	84.4	80.5	87.3	88.8	89.0	100
ZN9006	94.3	84.8	78.9	80.8	84.0	84.2	100
ZN9007	92.0	85.8	82.4	82.9	84.3	85.5	100
(B) Novel zinc electrodes made from electrochemical impregnation							
ZN9008	126.4	84.5	83.9	74.4	64.9	70.6	100
ZN9009	269.1	188.7	190.0	185.5	160.2	155.3	200
ZN9010	259.5	189.3	181.5	159.1	154.0	162.0	200
ZN9011	261.3	178.9	169.9	146.3	139.2	165.2	200
ZN9012	265.4	191.6	165.5	145.6	138.4	158.4	200
ZN9013	235.4	200.9	149.8	142.1	156.0	184.2	200

[a] Capacity was measured at a 0.375 C discharge rate and a C/3 charge rate with 150 mAh (nos. 1–8) and 300 mAh (nos. 9–13) charge input.

Table 5
Parameters of 670 mAh accordion-fold Ni–Zn cell

Cell number	NiZn-05
Electrode working area (cm^2)	60
Fold feature	Five folds of a laminate of 6 cm × 2 cm dimensions
Rated cell capacity (0.2 C discharge) (mAh)	670
Separators	Three-layer Celgard 3401 and two-layer Pellon 2517
Operation pressure	0–8 psi, stabilized at about 1.0 psi after 15 cycles
Electrolyte saturation level	70% ESL

3.4. Nickel–zinc cells with accordion-fold structures

The sample of the NiZn-05 accordion-fold cell (670 mAh rated capacity, 0.2 C discharge) was assembled with five accordion folds. Nickel and zinc electrodes in the nickel–zinc cell had an electrode thickness of 0.43 mm and 0.30 mm, respectively. The nickel fiber preform was put onto an expended nickel mesh. The mesh was 38 μm thick. The finished nickel electrode had a capacity of 763 mAh in the half-cell after 10 formation cycles. The copper substrate was made from 6 μm copper fiber and a copper expended mesh and had a thickness of 0.20 mm. After electro-precipitation, the thickness of zinc electrode increased to 0.30 mm. The theoretical capacity of zinc electrode was 2200 mAh. Three layers of Celgard 3401 and two layers of Pellon 2517 were used as cell separators. Zinc electrodes were to be made of sintered copper microfibrous substrates and coated with cadmium or lead to minimize hydrogen gassing. The nickel electrodes were to have a specific capacity of approximately 10 mAh/cm^2.

The cell test results were shown in Figs. 7 and 8. During the 14 and 15 cycles, the test cell was reconditioned for

Table 6
Comparison of a thin electrode accordion-fold cell and a thick electrode single Ni–Zn cell (two cells had a designed 600 mAh capacity)

Cell type and name	Accordion-fold cell (NiZn-05)	Thick electrode cell (NiZn-07a)
Cell rated capacity (mAh)	670 (0.18 C discharge)	483 (0.25 C discharge)
Charge and discharge current (mA)	200	200
Electrode working area (cm^2)	60	12
Nickel electrode thickness (mm)	0.43	2.10
Zinc electrode thickness (mm)	0.30	1.98
Electrode dimension after assembly (mm^3)	60 × 20 × 3.66	60 × 20 × 4.08
Maximum voltage during charge (V)	1.950	2.249
Maximum end-of-discharge voltage (V)	1.655	1.448
Average voltage of EOCV (end-of-charge voltage) (V)	1.920	2.107
Average voltage of EODV (end-of-discharge voltage) (V)	1.526	1.391
Coulomb efficiency (%)	96.7	91.0
Energy efficiency (%)	86.6	77.6
Cycle number	158	20

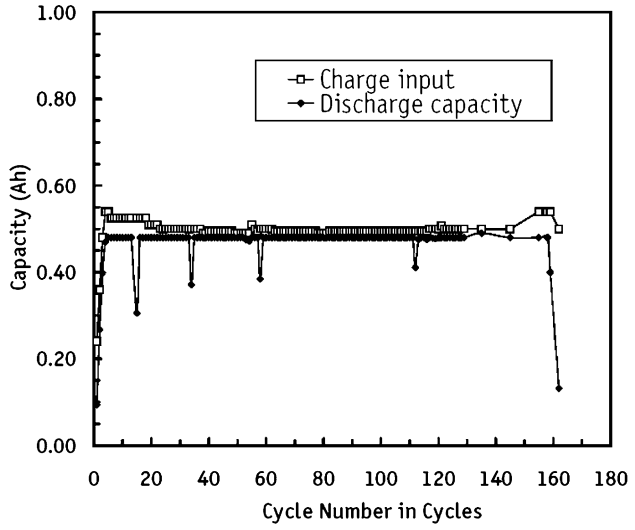

Fig. 7. Charge and discharge capacities vs. cycle number of the NiZn-05 accordion-fold cell (670 mAh rated capacity) made from microfibrous nickel and zinc electrodes. Cell charge/discharge at 0.3 C rates and 72% DOD.

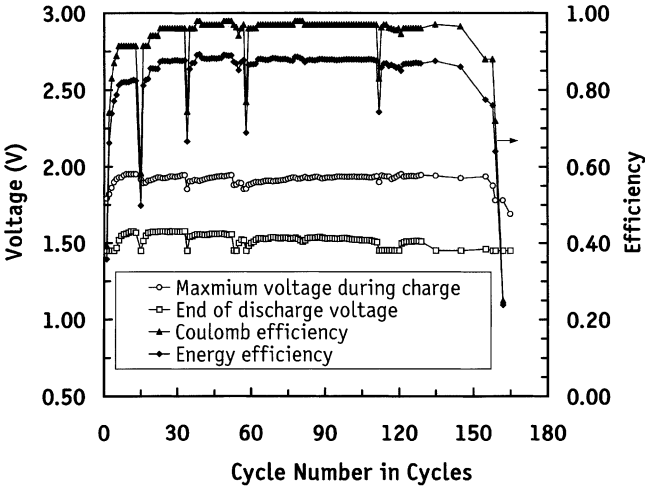

Fig. 8. Coulomb and energy efficiency vs. cycle number of the NiZn-05 accordion-fold cell made from microfibrous nickel and zinc electrodes. Cell charge/discharge at 0.3 C rates and 72% DOD.

further cell cycling. It was completely charged and discharged to adjust its working duration. The discharge capacity was stabilized at 480 mAh at a 0.3 C discharge rate. The cell had a 1.93 V maximum end-of-charge voltage and a 1.58 V end-of-discharge voltage after 30 cycles. Meantime, the cell's coulomb efficiency was 96% and energy efficiency was 88% when it was cycled at 72% DOD with a 74.6% SOR. Its coulomb efficiency was 98.0%, and energy efficiency was 88.6% at 72% DOD and a 73.2% SOR in the 79th cycle. The nickel–zinc cell needed to be reconditioned after a period of cycle testing. In the 127th cycle, the cell had a 1.936 V maximum voltage during charge and a 1.513 V end-of-discharge voltage (EODV). Its coulomb efficiency was still 96.0%, and energy efficiency was 87.0% at a 72% DOD and an 74.6% SOR. The 670 mAh nickel–zinc cell was made that completed the 158th cycle at 72% DOD and failed after the 159th cycle. After the cell finished its cycle test, it was opened and analyzed. It was understood that the cell short was due to the cell edges and zinc redistribution. During the cycle test, zinc electrode materials were gradually built up inside the separators and slowly migrated toward the nickel electrode. This resulted in the cell having less efficiency. After the 155th cycle, the maximum voltage during charge was rapidly decreased as shown in Fig. 8. It demonstrated the build-up of zinc material between the positive and negative electrodes. During initial cycle stage, zinc electrode had good performance for oxygen recombination. The cell gas was mainly hydrogen. During the cycle test, the passivation of zinc electrode from shape change resulted in efficiency reduction of the zinc electrode. Fully charged nickel electrode produce more oxygen and reduce the capacity of zinc electrode. The cell rate performance was thus poor and it was difficult to operate at a higher depth-of-discharge.

The NiZn-30 accordion-fold cell (1279 mAh rated capacity, 0.3 C discharge) was assembled with an improved zinc electrode. The zinc electrode was electrochemically impregnated in a solution of 1.6 M $Zn(NO_3)_2$, 0.788 M $Ca(NO_3)_2$, and 0.10 M $NaNO_2$. The substrate consisted of sintered 6 μm copper fibers with a copper mesh support. The microfibrous substrate was first electroplated with lead at 2 mA/cm^2 for 20 min before impregnation. The finished zinc electrode contained a small amount of calcium and lead additives via this co-deposition method. The comparison of several zinc electrodes is shown in Fig. 6. Lead plating at a low current density (Fig. 5b–d) improved the electrode structure and increased the uniformity of the coating layer. Two more layers of Celgard 5401 were applied to increase the electrode wetting ability. The cell was activated via the formation procedure using 20% KOH solution, and then was continuously tested in the same KOH solution after the excess electrolyte in the cell was drained.

The above cell had a 1263 mAh measured capacity during cycles 5–38. The cell was cycled at 38% DOD (Figs. 9 and 10). It was charged at a 0.45 C rate for approximate 55 min and discharged at a 0.65 C rate for 35 min. The cell's capacity was measured at a 0.3 C discharge rate after it was charged at a 0.3 C rate between 84.4 and 100.9% SOR. The coulomb efficiency was 94.5%, and the energy efficiency was 76.1% at 38% DOD and a 38.7% SOR in the 79th cycle. At cycle 185, the cell performance was poor at 38% DOD. The cell reconditioning was performed through discharging the nickel electrode to an additional hydrogen electrode. The cell was also conditioned at cycles 324, 707, and cycle 763. After cycle 836, the cell was still operated at 38% DOD but use of 0.16 C charge and discharge rates instead. After 1050 cycles, the cell capacity was hard to recover for further test at 38% DOD and reached its end-of-life.

The sample of the NiZn-20 accordion-fold cell (7115 mAh rated capacity, 0.08 C discharge) consisted of

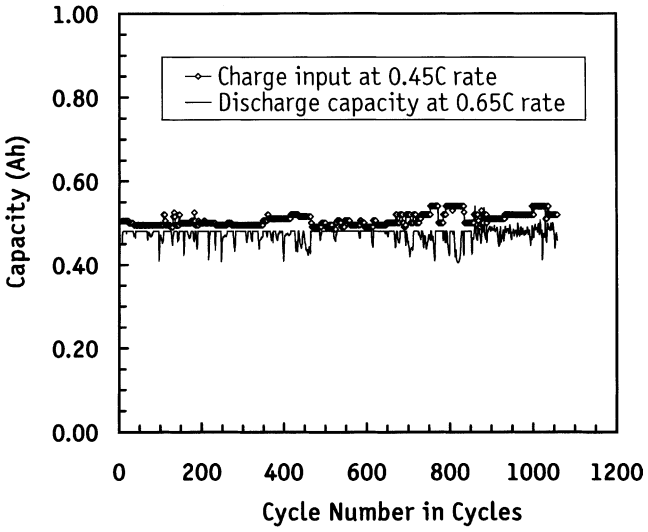

Fig. 9. Charge and discharge capacities vs. cycle number of the NiZn-30 accordion-fold cell (1279 mAh rated capacity) made from microfibrous nickel and zinc electrodes at 38% DOD. Charge input at 0.45 C rate for approximate than 55 min and discharge at 0.65 C rate for 35 min.

six folds of a 20 cm × 30 cm anode/separator/cathode laminate. One fold of the cell had an area of 20 cm × 5 cm and six folds together had a 600 cm^2 geometric anode (cathode) area. Six microfibrous nickel electrodes were put between a 31.8 cm × 20 cm expended nickel mesh and Pellon, and then sealed at the edges with Celgard strips. Six segments of zinc electrodes were put between a copper mesh and Pellon, and then sealed at the edges with Celgard strips. The accordion-fold cell was assembled by folding two groups of electrode segments separated by three layers of Celgard. A layer of Pellon was sandwiched between two layers of Celgard for increasing the wetting ability and improving the cell cycle life. An additional nickel electrode was used to balance the working nickel electrode and a hydrogen electrode used for gas management. All the components were assembled in a sealed acrylic casing. The cell was filled with NCP electrolyte and saturated using vacuum.

The cell was tested at 67% DOD from cycles 32–241. It was reconditioned by discharging the nickel electrode to the additional nickel electrode for 2–3 Ah at a 0.13 C rate. The cell was reconditioned at cycles 47, 63, 88, 129, 150, 168, 194, 198 and 237. After cell charge at cycle 129, the cell was fed with enough NCP electrolyte for electrolyte redistribution. Excess electrolyte was drained after vacuum treatment. The cell test was temporarily interrupted due to a computer hard drive problem. Once the battery testing system was restarted, the cycling resumed at cycle 151. The cell had 90.6% coulomb efficiency and 77.8% energy efficiency during cycle 160. Cell performance gradually decreased after cycle 177. The cell was partially successful operating at 67% DOD due to a shape change of the zinc electrode and reduced nickel electrode utilization.

The computer hard drive of the Arbin Battery Tester failed at cycle 151, and related data between cycles 47 and 150 was not recovered. An additional hard drive was applied to backup testing data frequently to prevent data loss in case of another hard-drive crashing. Mirror image data from Drive C was written to the additional back-up drive D. The working nickel electrode in the cell was connected with an additional nickel electrode for increasing nickel capacity during cycle 200. The cell capacity fluctuated when it was tested between cycles 178 and 241. Gas recombination was slower and cell pressure gradually built-up to 60 psi. Most of the cell gas was determined to be oxygen by measuring the voltages of Ni/H_2 and Zn/O_2 cells. These results showed that

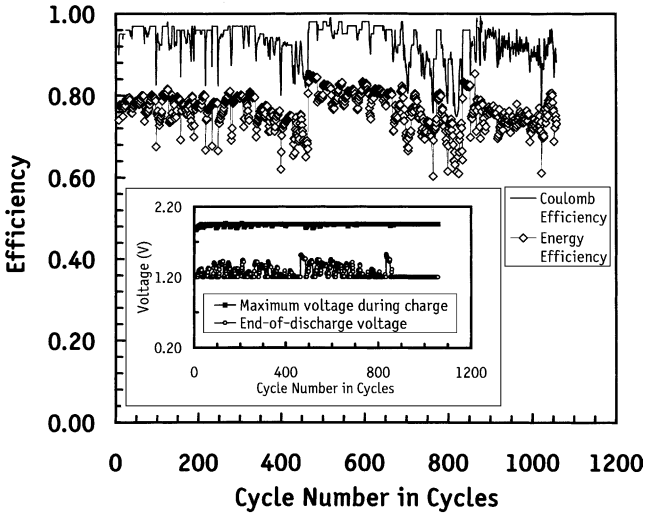

Fig. 10. Coulomb, energy efficiency, and voltage parameters vs. cycle number of the NiZn-30 accordion-fold cell made from microfibrous nickel and zinc electrodes at 38% DOD. Charge input at a 0.45 C rate and discharge at a 0.65 C rate.

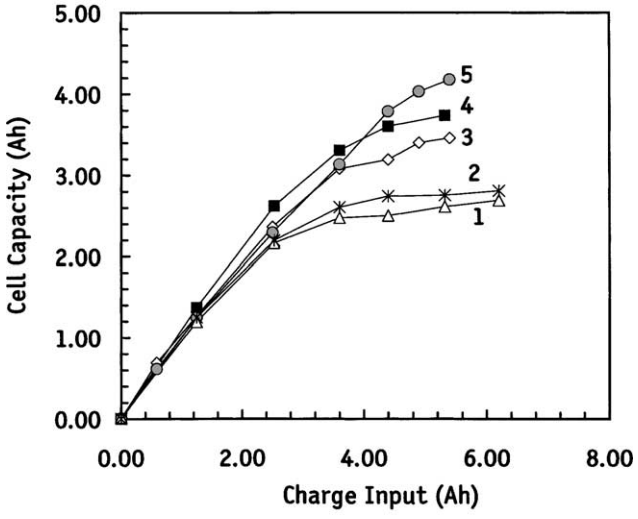

Fig. 11. The NiZn-20 cell capacity as a function of cell charge input at a 0.28 C charge rate and charge voltage no more than 1.95 V. (1) Discharge at 0.28 C rate after cycle 608; (2) discharge at 0.08 C rate after cycle 608; (3) discharge at 0.28 C rate after cycle 469; (4) discharge at 0.28 C rate after cycle 388; (5) discharge at 0.08 C rate after cycle 469.

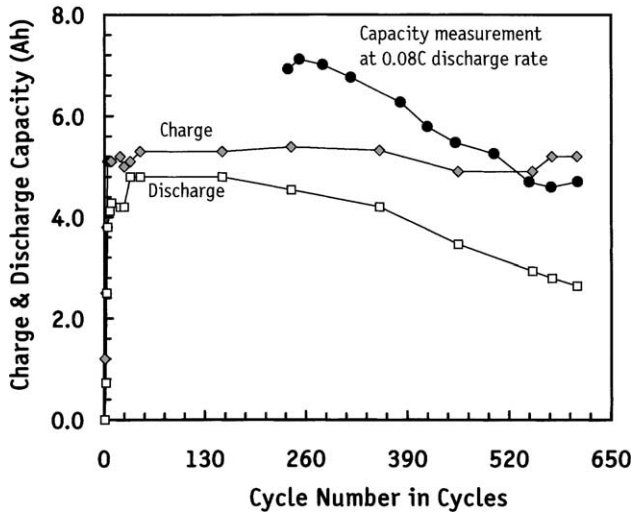

Fig. 12. Charge and discharge capacities vs. cycle number of the NiZn-20 accordion-fold cell (7115 mAh rated capacity) made from microfibrous nickel and zinc electrodes at 0.28 C charge and discharge rates.

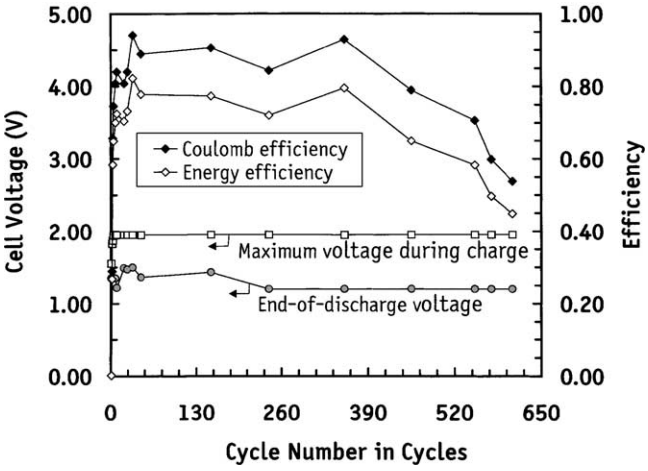

Fig. 13. Coulomb, energy efficiency, and voltage parameters vs. cycle number of the NiZn-20 accordion-fold cell made from microfibrous nickel and zinc electrodes at 0.28 C charge and discharge rates.

the zinc shape change (passivation) partially decreased cell performance. The cell was cycled again at 59% DOD between cycles 241 and 367. Test results are shown in Figs. 11–13. It was reconditioned by discharging the nickel electrode to an additional secondary nickel electrode for 2–3 Ah at a 0.13 C rate. After cycle 367, the cell capacity decreased quickly. The cell capacity then was reduced to about 3.40–3.50 Ah at a 0.28 C discharge rate. It had a 5.47 Ah capacity when the cell was discharged at a 0.08 C rate at cycle 452. The cell pressure fluctuated from 0 to 20 psi. The cell gas was determined primarily to be oxygen during the end-of-charge process by measuring the Zinc–O_2 cell voltage. The highest cell capacity was 7115 mAh during cycle 252 at a 0.08 C discharge rate. After cycle 469, test results demonstrated that rate performance was poorer at a 0.28 C discharge rate than at a 0.08 C discharge rate (Fig. 11). Its coulomb efficiency was 58.2% and energy efficiency was 47.2% at 44% DOD at the 478th cycle. The rated capacity 5.25 Ah was obtained during cycle 501. Its capacity and rate performance decreased gradually, as shown in Figs. 11 and 12. The cell was cycled at 37% DOD during the 607th cycle and had a 4.7 Ah rated capacity during the 608th cycle. The scale-up design and zinc electrode structure need further improvement for the larger 7 Ah accordion-fold batteries.

4. Conclusion

Newly developed microfibrous copper substrates are highly porous three-dimensional metallic support materials for active materials, such as zinc and zinc oxide or zinc electrodes. The three-dimensional microfibrous support structure with higher surface area and lightweight features can be applied to develop different types of electrodes and batteries for high energy and high power density applications. Coating or plating of a suitable metal film is necessary on microfibrous copper materials for zinc electrode applications.

Zinc electrodes using microfibrous copper substrates have been developed through an electrochemical impregnation process, which is similar to electrochemical impregnation of the lightweight nickel electrode. The porous electrode has low weight, higher surface area, and good electrical conductivity. A nickel–zinc cell (670 mAh rated capacity) was tested and obtained of 96.0% coulomb efficiency, 87.0% energy efficiency at a 72% DOD and a 74.6% SOR with 0.3 C charge/discharge rates in the 127th cycle. The constructed cell completed the 158th cycle at 72% DOD and had higher energy and coulomb efficiency.

The NCP electrolyte is better used in a zinc electrode cell without a calcium additive. For the zinc electrode cells with calcium additive, 20% KOH is preferred in cell formation and cycle testing. Zinc electrodes were successfully impregnated with conformal coatings with microfibrous copper substrates, representing a novel approach to zinc electrode fabrication. A new electrode design was developed for the accordion-fold cell. Instead of using one continuous strip of electrode material, five or ten segments separated slightly (0.8–1.0 mm), were sintered onto an expanded metal mesh 65 mm width. This combination was easily folded along the gaps between the segments. The Performance of a 1279 mAh accordion-fold cell was improved by using a suitable additive in the zinc electrode. The cell, operated at a 0.45 C rate and 0.65 C discharge rate, was tested for 835 cycles at 38% DOD. It finished after about 1050 cycles at 38% DOD and reached its EOL. The 7115 mAh accordion-fold demonstration cell was tested at 0.28 C charge/discharge rates for 608 cycles and still had 4.7 Ah capacity at a 0.08 C discharge rate. Shape change of the zinc electrode reduced its rate capability and accelerated zinc electrode passivation. The consequent loss of zinc electrode capacity, accelerated the capacity build-up of the nickel

electrode and eventually caused the nickel–zinc cell to fail. Therefore, the cell reconditioning for capacity balance was important for cell maintenance. The zinc electrode additive, state-of-charge/recharge, depth-of-discharge, electrolyte management, separator, cell design, test position, cycle regime, cell gas recombination, and cell reconditioning were important factors to the cycle life of the accordion-fold nickel–zinc batteries.

Acknowledgements

This project was funded by Electric Power Research Institute, Contract no. EPRI-WORP-8061-04. The authors wish to thank Mr. Ron Putt from Electric Fuel Corporation for his guidance and advice. The authors also wish to acknowledge contributions from Mr. Peter J. Durben and Mr. John D. Abner during the initial phases of this project. The authors thank Mr. Peter J. Durben for assistance in taking two SEM pictures.

References

[1] B.J. Tatarchuk, M.F. Rose, A. Krishnagopalan, J.N. Zabasaja, D. Kohler, Mixed fiber composite structures: high surface area-high conductivity mixtures, US Patent 5,080,963 (1992).
[2] B.J. Tatarchuk, M.F. Rose, A. Krishnagopalan, Mixed Fiber Composite structures: method of preparation, articles therefrom, and uses therefor, US Patent 5,102,745 (1992).
[3] D. Kohler, J.N. Zabasaja, A. Krishnagopalan, B.J. Tatarchuk, Metal–carbon composite electrodes from fiber precursors. I. Preparation of stainless steel–carbon composite electrodes, J. Electrochem. Soc. 137 (1990) 136–141.
[4] D. Kohler, J.N. Zabasaja, A. Krishnagopalan, B.J. Tatarchuk, Metal–carbon composite electrodes from fiber precursors. II. Electrochemical characterization of stainless steel–carbon structures, J. Electrochem. Soc. 137 (1990) 1750–1757.
[5] B.A. Johnson, R.E. Ferro, G.M. Swain, B.J. Tatarchuk, J. Power Sources 47 (1994) 251.
[6] P.K. Adanuvor, J.A. Pearson, B. Miller, Bruce J. Tatarchuk, D.L. Britton, in: Proceedings of the Space Electrochemical Research and Technology Conference, NASA Lewis Research Center, Cleveland, Ohio, NASA Conference Publication 3337, May 1995, pp. 11–21.
[7] M.E. Flanzer, Development and Characterization of Thin Microfiber based zinc electrodes for battery applications, Master Thesis, Auburn University, Auburn, March 1998.
[8] J.A. Keralla, Zinc electrode manufacture, in: A. Fleischer, J. Lander (Eds.), Zinc–Silver Oxide Batteries, Wiley, New York, 1971, pp. 183–197.
[9] F.R. McLarnon, E.J. Cairns, The secondary alkaline zinc electrode, J. Electrochem. Soc. 138 (1991) 645–664.
[10] S. Arouete, K.F. Blurton, H.G. Oswin, J. Electrochem. Soc. 116 (1969) 166.
[11] J. McBreen, Nickel/zinc batteries, J. Power Sources 51 (1994) 37–44.
[12] E.G. Gagnon, Y.-M. Wang, J. Electrochem. Soc. 134 (1987) 2091.
[13] A. Charkey, Sealed zinc secondary battery and zinc electrode therefor, US Patent 5,460,899 (1995).
[14] F. Cao, A. Charkey, K. Williams, Thermal behavior and end-of-life characteristics of the nickel–zinc battery, in: Proceedings of the 35th Intersociety Energy Conversion Engineering Conference, vol. 2, 2000, pp. 985–994.
[15] C. Schlatter, C. Comninellis, S. Muller, O. Haas, in: New Promising Electrochemical Systems for Rechargeable Batteries, Kluwer Academic Publishers, Amsterdam, 1996, pp. 131–141.
[16] R.L. Beauchamp, D.W. Maurer, T.D. O'Sullivan, Methods of producing electrodes for alkaline batteries, US Patent 4,032,697 (1977).
[17] C. Bleser, Positive electrode processing for Hughes Ni–H_2 cells, in: Proceedings of the Goddard Space Flight Center Battery Workshop, 1981, pp. 471–480.
[18] D.L. Britton, Performance of lightweight nickel electrodes, NASA Technical Memorandum 100,958 (1988).
[19] J.A. Dean, Lance's Handbook of Chemistry, 12th ed., McGraw-Hill, New York, 1979, pp. 5–8, 12.
[20] R.A. Sharma, Thermodynamic properties of a zinc/nickel oxide cell, in: D.A. Corrigan, A.H. Zimmerman (Eds.), Proceedings of the Symposium on Nickel Hydroxide Electrodes, vol. 90-4, The Electrochemical Society, Pennington, NJ, 1990, pp. 403–425.